

Supplementary Information for Measuring the Competition Between Bimolecular Charge Recombination and Charge Extraction in Organic Solar Cells under Operating Conditions

Michael C. Heiber,^{1,2,*} Takashi Okubo,³ Seo-Jin Ko,¹ Benjamin R. Luginbuhl,^{1,4} Niva A. Ran,^{1,4} Ming Wang,^{1,4} Hengbin Wang,⁵ Mohammad Afsar Uddin,⁶ Han Young Woo,⁶ Guillermo C. Bazan,^{1,4} and Thuc-Quyen Nguyen^{1,4,†}

¹Center for Polymers and Organic Solids, University of California, Santa Barbara, California 93106, USA

²Center for Hierarchical Materials Design (CHiMaD),
Northwestern University, Evanston, Illinois 60208, USA

³Kinki University, Osaka, Japan

⁴Department of Chemistry and Biochemistry, University of California, Santa Barbara, California 93106, USA

⁵Mitsubishi Chemical Center for Advanced Materials,

University of California, Santa Barbara, California 93106, USA

⁶Department of Chemistry, Korea University, Seoul 136-713, Republic of Korea

(Dated: May 24, 2018)

I. ADDITIONAL THEORY AND METHODS DETAILS

A. Measuring the Steady State Bimolecular Recombination Kinetics and Mobility

The overall current generated by the solar cell can be split into two components,

$$J(V) = J_G(V) - J_{br}(V), \quad (1)$$

where $J_G(V)$ is the effective generation current and $J_{br}(V)$ is the bimolecular recombination current. In the reverse bias saturation regime of the J-V curve, the charge carrier density is low enough such that the bimolecular recombination is negligible, and as a result, the effective generation current density can be described

$$J_G(V) = qLG(V), \quad (2)$$

where $G(V)$ is the bias-dependent effective free charge generation rate. This effective generation rate represents a complex summation of all first-order mechanisms including photon absorption, exciton dissociation yield, charge carrier separation, surface recombination, exciton-charge annihilation, and charge recombination with injected charges present near the Ohmic contacts. All of these effects can be accounted for by analyzing the photocurrent in the saturation regime. For the devices measured in this study, the saturation photocurrent could be empirically fit using a simple power law function,

$$J_G(V) = J_{ph,sat}(V) = J_0 + J_1[V_0 - V]^p, \quad (3)$$

where J_0 , J_1 , and p are fit parameters. By extrapolating this fit to zero effective voltage, one can determine the generation current density at any applied bias from short-circuit to open-circuit. Subtracting the calculated generation current from the total measured current, then yields the bimolecular recombination current.

$$J_{br}(V) = J_G(V) - J(V). \quad (4)$$

Alternatively, the bimolecular recombination current can also be defined,

$$J_{br}(V) = qLk_{br}(n, V)n(V)^2. \quad (5)$$

Then, by combining Eqns. 4 and Eqn. 5 the bimolecular recombination coefficient can be calculated,

$$k_{br}(n, V) = \frac{J_G(V) - J(V)}{qLn(V)^2}, \quad (6)$$

To determine the effective mobility of the charge carriers, we expand on the method developed by Albrecht *et al.*¹ The current density produced by a solar cell is dominated by the drift and diffusion current of electrons and holes traveling through the active layer,¹

$$J = n\mu_e \nabla E_{qF,e} + p\mu_h \nabla E_{qF,h} \quad (7)$$

where n is density of electrons, μ_e is the electron mobility, $\nabla E_{qF,e}$ is the gradient of the quasi Fermi level of the electrons, p is the hole density, μ_h is the hole mobility, and $\nabla E_{qF,h}$ is the gradient of the quasi Fermi level of the holes. At steady state, the electron and hole current densities must be equal, and assuming equal densities of electrons and holes ($n = p$) and approximately equal charge carrier mobilities ($\mu_{eff} = \mu_e \approx \mu_h$),

$$J = 2n\mu_{eff} \nabla E_{qF}. \quad (8)$$

The gradient of the quasi Fermi levels can be defined¹

$$\nabla E_{qF} = q \frac{[V_{oc} - V]}{L} \quad (9)$$

where q is the elementary charge constant, V_{oc} is the open-circuit voltage of the solar cell, V is applied bias, and L is the active layer thickness, which results in the final form,

$$J(V) = 2qn\mu_{eff} \frac{[V_{oc} - V]}{L}. \quad (10)$$

However, as discussed previously, both the mobility and charge carrier density are not constants, and so the effective mobility is more generally defined,

$$\mu_{eff}(n, V) = \frac{J(V)L}{2qn(V)[V_{oc} - V]} \quad (11)$$

B. Measuring the Charge Carrier Density with Impedance Spectroscopy

Impedance spectroscopy can be used to determine the charge carrier density in the solar cell under operating conditions by measuring the chemical capacitance (C_μ) due to the charge carriers in the active layer as a function of the internal voltage. The chemical capacitance of the charge carriers must be calculated from the total capacitance of the solar cell (C_{tot}) after subtracting the capacitance of the depleted device in the dark (C_d).

$$C_\mu = C_{\text{tot}} - C_d \quad (12)$$

Here, we measure C_d as a function of frequency at $V = -4$ or -5 V.

The total capacitance of the solar cell at a given bias and illumination intensity, after correcting for the series resistance and parasitic induction of the wires, is calculated

$$C_{\text{tot}} = -\frac{1}{\omega} \left[\frac{Z'' - \omega L_w}{[Z' - R_s]^2 + [Z'' - \omega L_w]^2} \right], \quad (13)$$

where ω is the angular frequency, Z' is the real impedance, Z'' is the imaginary impedance, L_w is the inductance of the wires, and R_s is the series resistance due to the wires and connection to the device electrodes. The angular frequency is related to the regular frequency (f) by $\omega = 2\pi f$.

At high frequency, in the dark, and at reverse bias, the complexities that make equivalent circuit modeling difficult largely disappear because there are very few charge carriers in the active layer and any that are present are unable to respond to the high frequency AC signal. As a result, the high frequency real impedance (Z') resulting from a simple RC circuit can be used to determine the series resistance.

$$Z'(f \approx 10^6 \text{ Hz}) = R_s \quad (14)$$

Under the same conditions, the high frequency imaginary impedance can then be used to determine the parasitic inductance of the wires (L_w) and the geometric capacitance of the device (C_g) by fitting the following equation

$$Z''(f \approx 10^6 \text{ Hz}) = \omega L_w - \frac{1}{\omega C_g} \quad (15)$$

With this measurement of the geometric capacitance, the effective dielectric constant of the active layer blend can then be calculated,

$$\epsilon = \frac{C_g L}{\epsilon_0 A}, \quad (16)$$

where ϵ_0 is the vacuum permittivity constant.

We now reassess the derivation for the equation used to calculate the saturation charge carrier density (n_{sat}) Originally, Proctor *et al.* used the expression,²

$$n_{\text{sat}}(V_{\text{sat}}) = \frac{1}{qAL} C_\mu(V_{\text{sat}}) [V_0 - V_{\text{sat}}], \quad (17)$$

In the original derivation, only the drift current of one type of carrier was included,² disregarding the fact that both charge carrier types contribute to the total current density and the possible contribution from charge carrier diffusion. Instead, here we start by using the more complete drift-diffusion current defined in Eqn. 10, In the saturation regime, Eqns. 10 and 2 can be set equal to each other and rearranged to give the saturation charge carrier density.

$$n_{\text{sat}}(V) = \frac{L^2 G}{2\mu_{\text{eff}}[V_{\text{oc}} - V]} \quad (18)$$

While we do not know the generation rate or the mobility, we can measure the capacitance. Given that capacitance equation is

$$C_\mu(V) = qAL \frac{dn}{dV}, \quad (19)$$

we can take the derivative of Eqn. 18 to simply the expression. If G and μ_{eff} are independent of the applied bias,

$$\frac{dn_{\text{sat}}(V)}{dV} = \frac{L^2 G}{2\mu_{\text{eff}}[V_{\text{oc}} - V]^2} \quad (20)$$

and combining this with Eqn. 18,

$$\frac{dn_{\text{sat}}(V)}{dV} = \frac{n_{\text{sat}}(V)}{[V_{\text{oc}} - V]} \quad (21)$$

Combining this with Eqn. 19, we reach a the general expression for n_{sat} at a saturation voltage V_{sat} ,

$$n_{\text{sat}}(V_{\text{sat}}) = \frac{1}{qAL} C_\mu(V_{\text{sat}}) [V_{\text{oc}} - V_{\text{sat}}], \quad (22)$$

and this equation can then be used to calculate the saturation carrier density at any bias in the reverse saturation regime. The only difference between the original equation (Eqn. 17) derived by Proctor *et al.* is that V_{oc} has been substituted for V_0 due to the addition of the contribution from the diffusion current. In most cases, $V_{\text{oc}} \approx V_0$, and this difference will only have a small impact on n_{sat} .

However, if G and μ_{eff} are not independent of the applied bias, then this equation will not be strictly valid. A more detailed derivation of n_{sat} can take these effects into account. In this case, the derivative of Eqn. 18 has a more complex form that can then be simplified to obtain a more complete expression for n_{sat} .

First, using the product rule for derivatives,

$$\frac{dn_{\text{sat}}(V)}{dV} = \left[\frac{L^2}{2[V_{\text{oc}} - V]} \right]' \frac{G(V)}{\mu_{\text{eff}}(V)} + \frac{L^2}{2[V_{\text{oc}} - V]} \left[\frac{G(V)}{\mu_{\text{eff}}(V)} \right]' \quad (23)$$

Then, using the quotient rule for derivatives,

$$\frac{dn_{\text{sat}}(V)}{dV} = \left[\frac{L^2}{2[V_{\text{oc}} - V]} \right]' \frac{G(V)}{\mu_{\text{eff}}(V)} + \frac{L^2}{2[V_{\text{oc}} - V]} \left[\frac{G(V)' \mu_{\text{eff}}(V) - G(V) \mu_{\text{eff}}'(V)}{\mu_{\text{eff}}(V)^2} \right] \quad (24)$$

This then becomes

$$\frac{dn_{\text{sat}}(V)}{dV} = \frac{L^2}{2[V_{\text{oc}} - V]^2} \frac{G(V)}{\mu_{\text{eff}}(V)} + \frac{L^2}{2\mu_{\text{eff}}(V)^2 [V_{\text{oc}} - V]} \left[\mu_{\text{eff}}(V) \frac{dG(V)}{dV} - G(V) \frac{d\mu_{\text{eff}}(V)}{dV} \right] \quad (25)$$

After simplifying by plugging in Eqn. 18,

$$\frac{dn_{\text{sat}}(V)}{dV} = \frac{n_{\text{sat}}(V)}{[V_{\text{oc}} - V]} + \frac{n_{\text{sat}}(V)}{G(V) \mu_{\text{eff}}(V)} \left[\mu_{\text{eff}}(V) \frac{dG(V)}{dV} - G(V) \frac{d\mu_{\text{eff}}(V)}{dV} \right] \quad (26)$$

Further simplification then leads to

$$\frac{dn_{\text{sat}}(V)}{dV} = \frac{n_{\text{sat}}(V)}{[V_{\text{oc}} - V]} + n_{\text{sat}} \left[\frac{1}{G(V)} \frac{dG(V)}{dV} - \frac{1}{\mu_{\text{eff}}(V)} \frac{d\mu_{\text{eff}}(V)}{dV} \right] \quad (27)$$

Substituting in the capacitance equation (Eqn. 19), solving for n_{sat} , setting letting $V = V_{\text{sat}}$ finally yields

$$n_{\text{sat}}(V_{\text{sat}}) = \frac{C_{\mu}(V_{\text{sat}})}{qAL} \left[\frac{1}{(V_{\text{oc}} - V_{\text{sat}})} + \frac{1}{G(V_{\text{sat}})} \frac{dG}{dV} - \frac{1}{\mu_{\text{eff}}(V_{\text{sat}})} \frac{d\mu_{\text{eff}}(V_{\text{sat}})}{dV} \right]^{-1} \quad (28)$$

In this equation, the second and third terms in the brackets modify n_{sat} to account for the possibility of a field-dependent effective charge generation rate or a field-dependent charge carrier mobility, respectively. In the simple case where these parameters are independent of the applied bias, these two terms are equal to zero and Eqn. 22 is regained. Since we do not know the effective generation rate, we can modify this equation further given that

$$G(V_{\text{sat}}) = \frac{J_{\text{G}}(V_{\text{sat}})}{qL} \quad (29)$$

and

$$\frac{dG(V_{\text{sat}})}{dV} = \frac{1}{qL} \frac{dJ_{\text{G}}(V_{\text{sat}})}{dV}. \quad (30)$$

Eqn. 28 can then be re-written as a function of the measured saturation current

$$n_{\text{sat}}(V_{\text{sat}}) = \frac{C_{\text{sat}}}{qAL} \left[\frac{1}{(V_{\text{oc}} - V_{\text{sat}})} + \frac{1}{J_{\text{G}}(V_{\text{sat}})} \frac{dJ_{\text{G}}(V_{\text{sat}})}{dV} - \frac{1}{\mu_{\text{eff}}(V_{\text{sat}})} \frac{d\mu_{\text{eff}}(V_{\text{sat}})}{dV} \right]^{-1} \quad (31)$$

C. Measuring Bimolecular Charge Recombination with the Open-Circuit Voltage Decay Technique

The relationship between the measured V_{oc} and the charge carrier density in classical semiconductor theory is

$$qV_{\text{oc}} = E_{\text{g}} + k_{\text{B}}T \ln \left[\frac{np}{N_{\text{e}}N_{\text{h}}} \right], \quad (32)$$

where E_{g} is the bandgap of the semiconductor, k_{B} is the Boltzmann constant, T is the temperature, N_{e} is the total density of electron states, and N_{h} is the total density of hole states.

In OPVs, the relationship between the measured open-circuit voltage (V_{oc}) and the charge carrier density has been shown to depend on the charge transfer state energy (E_{CT}) and further modified by energetic disorder. Organic semiconductors are disordered materials and have a broadened density of states (DOS) with a tail

that extends into the bandgap, and it has been shown that the open-circuit voltage is reduced relative to the charge transfer state energy depending on the nature and amount of disorder.^{3,4} If the DOS tail has a Gaussian shape,

$$qV_{oc} = E_{CT} - \frac{\sigma^2}{k_B T} + k_B T \ln \left[\frac{np}{N_e N_h} \right], \quad (33)$$

where σ is the standard deviation of the Gaussian DOS. If the DOS tail has an exponential shape,

$$qV_{oc} = E_{CT} + mk_B T \ln \left[\frac{np}{N_e N_h} \right]. \quad (34)$$

where

$$m = \frac{E_u}{k_B T} \quad (35)$$

and E_u is the characteristic Urbach energy of the exponential tail.

For a blend with an unknown DOS shape, both the Gaussian and exponential DOS model equations can be generalized to the form

$$V_{oc} = E_0 + \frac{m_d k_B T}{q} \ln np. \quad (36)$$

where E_0 is a fit parameter and m_d is the disorder prefactor.

II. ADDITIONAL EXPERIMENTAL DETAILS AND RESULTS

Figure 1 shows the chemical structures for all of the polymer donors and fullerene acceptors used in this study.

In total, 34 devices were tested using the full impedance-photocurrent device analysis (IPDA) and open-circuit voltage decay (OCVD) methods. For each device, detailed information about the materials used, the fabrication process, the final device dimensions, 1 sun J - V characteristics, and 1 sun results from IPDA and OCVD measurements can be found in the Supplementary Data spreadsheet that accompanies this document. Illumination intensity data can be made available for further analysis upon request.

For some of the P3HT:PC₆₁BM devices, a slow drying/solvent vapor annealing process was used. This was done by spin coating the film for only 10s and then quickly placing substrate with the still wet film into an empty covered glass petri dish for 10 min. Once in the covered petri dish, the film continued to dry and the solvent vapor populated the atmosphere of the petri dish, thereby increasing the partial pressure of the environment and slowing down the evaporation of the solvent from the film. After the 10 min slow drying step, the films were exposed to the N₂ glovebox environment and allowed to complete drying for 1 hr.

* heiber@mailaps.org

† quyen@chem.ucsb.edu

¹ S. Albrecht, J. R. Tumbleston, S. Janietz, I. Dumsch, S. Allard, U. Scherf, H. Ade, and D. Neher, *J. Phys. Chem. Lett.* **5**, 1131 (2014).

² C. M. Proctor, C. Kim, D. Neher, and T.-Q. Nguyen, *Adv.*

Funct. Mater. **23**, 3584 (2013).

³ J. C. Blakesley and D. Neher, *Phys. Rev. B* **84**, 075210 (2011).

⁴ I. Lange, J. Kniepert, P. Pingel, I. Dumsch, S. Allard, S. Janietz, U. Scherf, and D. Neher, *J. Phys. Chem. Lett.* **4**, 3865 (2013).

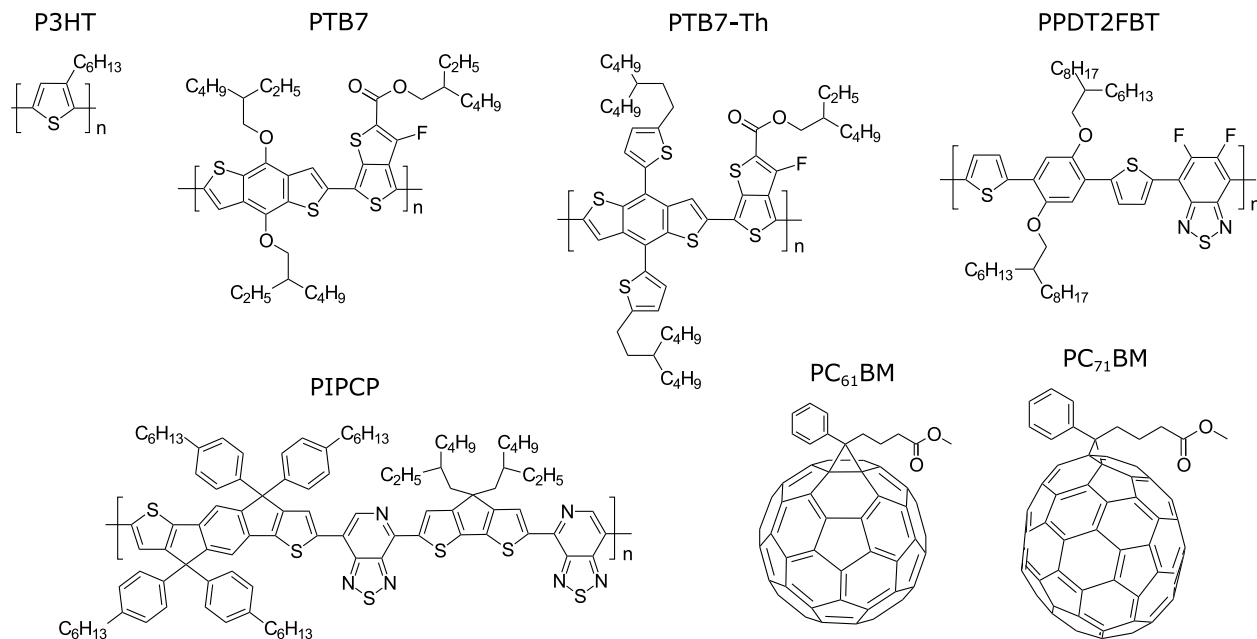


FIG. 1. Chemical structures of the polymer donors (P3HT, PTB7, PTB7-Th, PPDT2FBT, PIPCP) and the fullerene acceptors (PC₆₁BM, PC₇₁BM).